ORIGINAL ARTICLE

Fur glowing under ultraviolet: *in situ* analysis of porphyrin accumulation in the skin appendages of mammals

Séverine L. D. TOUSSAINT,[1] Jasper PONSTEIN,[2,3] Mathieu THOURY,[4] Rémi MÉTIVIER,[5] Daniela C. KALTHOFF,[6] Benoît HABERMEYER,[7] Roger GUILARD,[8] Steffen BOCK,[2] Peter MORTENSEN,[6] Sverre SANDBERG,[9] Pierre GUERIAU[4,10] and Eli AMSON[11]

[1]AG Vergleichende Zoologie, Institut für Biologie, Humboldt Universität zu Berlin, Berlin, Germany, [2]Museum für Naturkunde Berlin, Leibniz Institute for Evolution and Biodiversity Science, Berlin, Germany, [3]AG Paläobiologie und Evolution, Institut für Biologie, Humboldt Universität zu Berlin, Berlin, Germany, [4]IPANEMA, CNRS, ministère de la Culture, UVSQ, MNHN, USR3461, Université Paris-Saclay, Gif-sur-Yvette, France, [5]Université Paris-Saclay, ENS Paris-Saclay, CNRS, PPSM, Gif-sur-Yvette, France, [6]Department of Zoology, Swedish Museum of Natural History, Stockholm, Sweden, [7]PorphyChem SAS, Dijon, France, [8]ICMUB, UMR CNRS 6302, Université de Bourgogne Franche-Comté, France, [9]Norwegian Porphyria Centre (NAPOS), Haukeland University Hospital, Norwegian Organization for Quality Improvement of Laboratory Examinations (Noklus), and Department of Global Public Health and Primary Care, Faculty of Medicine, University of Bergen, Norway, [10]Institute of Earth Sciences, University of Lausanne, Lausanne, Switzerland and [11]Staatliches Museum für Naturkunde Stuttgart, Stuttgart, Germany

Abstract

Examples of photoluminescence (PL) are being reported with increasing frequency in a wide range of organisms from diverse ecosystems. However, the chemical basis of this PL remains poorly defined, and our understanding of its potential ecological function is still superficial. Among mammals, recent analyses have identified free-base porphyrins as the compounds responsible for the reddish ultraviolet-induced photoluminescence (UV-PL) observed in the pelage of springhares and hedgehogs. However, the localization of the pigments within the hair largely remains to be determined. Here, we use photoluminescence multispectral imaging emission and excitation spectroscopy to detect, map, and characterize porphyrinic compounds in skin appendages *in situ*. We also document new cases of mammalian UV-PL caused by free-base porphyrins in distantly related species. Spatial distribution of the UV-PL is strongly suggestive of an endogenous origin of the porphyrinic compounds. We argue that reddish UV-PL is predominantly observed in crepuscular and nocturnal mammals because porphyrins are photodegradable. Consequently, this phenomenon may not have a specific function in intra- or interspecific communication but rather represents a byproduct of potentially widespread physiological processes.

Key words: *in situ* analysis, mammal, multispectral imaging, porphyrin, UV photoluminescence

Correspondence: Jasper Ponstein, AG Paläobiologie und Evolution, Institut für Biologie, Humboldt Universität zu Berlin, Invalidenstraße 43, Nordbau, 10115 Berlin, Germany.

Email: ponsteij@hu-berlin.de

Séverine L. D. Toussaint and Jasper Ponstein are co-first authors.

INTRODUCTION

Ultraviolet-induced photoluminescence (UV-PL) has been described in the external organs of plants (Lagorio *et al.* 2015), "invertebrates" (Jeng 2019), and in numerous vertebrates, including "fishes," lissamphibians, squamates, birds, and mammals (Prötzel *et al.* 2021). As far as mammals are concerned, only a handful of observations have been reported, notably in the platypus (Anich *et al.* 2021), in marsupials including opossums (Meisner 1983; Pine *et al.* 1985; Tumlison & Tumlison 2021) and bandicoots (Reinhold 2021), in weasels (Latham 1953; Tumlison & Tumlison 2021), in rodents including flying squirrels (Kohler *et al.* 2019), springhares (Olson *et al.* 2021), and pocket gophers (Pynne *et al.* 2021), and in hedgehogs (Derrien & Turchini 1925; Hamchand *et al.* 2021; Silpa *et al.* 2021).

Interestingly, this UV-PL can occur in different tissues, and its observed colors vary widely within the visible spectrum depending on the species considered. Reported colors include shades of dark blue or violet for bones (Bachman & Ellis 1965; Moncrief & Dooley 2013; Taboada *et al.* 2017; Prötzel *et al.* 2018; Goutte *et al.* 2019), of light blue and green for skin and hair (Pine *et al.* 1985; Taboada *et al.* 2017; Kohler *et al.* 2019; Anich *et al.* 2021; Prötzel *et al.* 2021), of yellow for feathers (e.g. Pearn *et al.* 2001; Arnold *et al.* 2002; McGraw *et al.* 2007), and shades of pink to red from feathers as well as from the pelage of most of the photoluminescent mammals (Meisner 1983; Pine *et al.* 1985; Weidensaul *et al.* 2011; Kohler *et al.* 2019; Hamchand *et al.* 2021; Silpa *et al.* 2021; Olson *et al.* 2021; Reinhold 2021). This high variability implies that several UV-reactive molecular or structural compounds contribute to this phenomenon. For example, biological fluids like urine are known to be photoluminescent (Leiner *et al.* 1987; Kellie *et al.* 2004), resulting in blue to yellow UV-PL. Recent studies found that iridophores in the dermis of a gecko can produce greenish UV-PL (Prötzel *et al.* 2021). The reddish UV-PL observed on the plumage of some birds was identified as caused by coproporphyrin III and protoporphyrin IX (Church & Oxon 1869; Rimington 1939; Negro *et al.* 2009; Galván *et al.* 2016; Camacho *et al.* 2019; Okazaki & Imamura 2019), which are common molecules that play a crucial role in various biological processes, notably in heme biosynthesis (Ajioka *et al.* 2006; Tahoun *et al.* 2021). Recent analyses of the hair of springhares (*Pedetes* sp.) (Olson *et al.* 2021) and the spines of the European hedgehog (*Erinaceus europaeus*) (Hamchand *et al.* 2021) identified a mixture of free-base porphyrins that are usually found in the urine or feces of mammals (Rimington & Moore 1985). However, the compounds responsible for the UV-PL observed in other mammals remain unidentified. Moreover, the precise spatial distribution of photoluminescent compounds within the skin appendages (i.e. hair and spines) is largely unknown. Answering these questions would greatly improve our understanding of the biological origin, either endogenous or exogenous (Hamchand *et al.* 2021), and the potential function of such photoluminescence mechanism.

In addition to the molecular identification and precise localization of the pigments, it remains unclear whether UV-PL is actually perceived and acted upon by the organisms in their natural environment (Lagorio *et al.* 2015; Marshall & Johnsen 2017). So far, 2 cases of sexual selection involving PL have been experimentally demonstrated in budgerigars (Arnold *et al.* 2002) and jumping spiders (Lim *et al.* 2007). In mammals, based on the fact that UV-PL is predominantly observed in crepuscular or nocturnal animals, it was recently hypothesized that it could serve ecological functions in light-deprived environments such as intraspecific communication or camouflage (Kohler *et al.* 2019; Anich *et al.* 2021; Olson *et al.* 2021). These hypotheses have not been tested experimentally and have since been challenged (Hamchand *et al.* 2021; Hughes *et al.* 2022). Moreover, because the species concerned live in a wide range of ecosystems and differ widely in life histories, from the semi-aquatic platypus to the terrestrial springhares and the arboreal flying squirrels, it remains unclear whether UV-PL has indeed a specific ecological significance in nocturnal animals, or is simply incidental to other physiological processes (Lagorio *et al.* 2015; Marshall & Johnsen 2017; Hamchand *et al.* 2021; Hughes *et al.* 2022).

Here, we use UV-PL multispectral imaging and spectroscopy to identify and localize *in situ* the organic compounds responsible for the reddish UV-PL observed in most of the species' pelage as free-base porphyrins. Our results support the notion that the accumulation of free porphyrins into mammalian pelage, resulting in an observable photoluminescence under UV illumination, is endogenous and ubiquitous in distantly related therian species in both major subclades, that is, marsupials and placental mammals. We further suggest that this phenomenon could be a by-product of the excretion of porphyrins to the pelage and that it may have little to do with a specific function in nocturnal communication as previously argued.

Terminological clarifications

Photoluminescence is a physical phenomenon in which a material reemits photons after a photonic excitation.

It encompasses 2 distinct phenomena, namely fluorescence and phosphorescence, which differ in the electronic states involved in the radiative de-excitation pathway. Fluorescence and phosphorescence occur when the molecule in an excited state returns to its electronic ground state (essentially S_0 for most organic molecules) from an excited singlet or triplet state, respectively, by emission of a photon. The fluorescence process occurs within a few tens of picoseconds to a few hundreds of nanoseconds, whereas phosphorescence, which corresponds to the forbidden transition between the excited and ground states, takes place on timescales than can span from microseconds to minutes or more. UV-induced photoluminescence (UV-PL) is the process whereby absorbed UV photons trigger a radiative de-excitation at longer wavelengths. In contrast, bioluminescence (BL) corresponds to the emission of light generated by a living organism via chemical reactions.

Multiple cases of UV-PL and BL have been observed in various organisms either in their natural habitat or from preserved museum specimens. Unfortunately, UV-PL is often referred to as "biofluorescence" in the literature, which might confuse the scientific community as well as the general public. We prefer to use UV-PL in this context, because it is still unclear whether it is fluorescence or phosphorescence that is involved, and also to distinguish it from bioluminescence. Moreover, although both phenomena result in spectacular luminous or glowing organisms, they result from quite different mechanisms and do not occur under the same conditions. In practice, the UV-PL phenomenon is only observable to the human eye through the use of an artificial source of ultraviolet light, in combination with an optical filter to ensure error-free visual interpretation. Importantly, BL can be correlated to identifiable functions, whereas PL and UV-PL phenomena are more difficult to functionally interpret (Marshall & Johnsen 2017).

MATERIALS AND METHODS

Specimens studied

We examined specimens of several species of monotremes, marsupials, and placental mammals with preserved furs in either alcohol or as dry preparations, from museum collections of the Museum für Naturkunde of Berlin, the Swedish Museum of Natural History of Stockholm, the Muséum national d'Histoire naturelle of Paris, the JAGUARS collection of Cayenne, the personal collection from Dr. Anthony Herrel, and the Naturkundemuseum of Potsdam. A selection of specimens and associated methods of analysis are listed in Table 1.

To proceed with photoluminescence spectroscopy and multispectral imaging, we collected several samples of complete hairs and spines of known orientation and localization on the pelage of several selected specimens (Table 1 and Figs 1a,2a). We also carried out spectroscopy and multispectral imaging measurements on 2 complete specimens preserved in alcohol (JAGUARS-M535 and JAGUARS-M2838).

UV-induced photoluminescence macro-analysis and photography

We first observed and photographed specimens under natural or standard white light conditions. Subsequently, we placed the specimens in the dark and illuminated them using specific UV light setups emitting from a distance of about 20 cm from the specimens. We initially used a 395-nm LED torch (100 LED flashlight, Youthink) following Kohler et al. (2019) combined with a yellow filter (K&F Concept) to absorb the purple light emitted by the torch. Nevertheless, this setup may have left out wavelengths that are not absorbed by the yellow filter and which could be misinterpreted as UV-PL. We therefore used a professional 365-nm compact lamp (4 W, UVL-21, UVP) equipped with a strict UV black filter (Filter Band U-360 2IN SQ, Edmund Optics Ltd). Photographs presented in Fig. 1a were obtained using the second setup, with the filter placed directly on the UV-emitting surface of the lamp. We took photographs using a Canon EOS 5D Mark III equipped with a 50-mm macro lens and a UV blocking filter (UV390 Protect Filter, Hama). White balance was systematically readjusted for each specimen.

Photoluminescence spectroscopy

We performed emission and excitation spectroscopy using a Fluorolog 3–22 spectrofluorometer (HORIBA Jobin Yvon). We collected spectra using a bundle of optical fibers equipped with focusing optics to perform measurements out of the analysis compartment. We set the entrance and exit slits widths of the monochromators to 10 nm in order to ensure a balance between the collection of spectra with good signal-to-noise and a spectral resolution compatible with the detection of Q-bands. We then collected emission spectra using an excitation at 400 nm. To record the excitation spectra, we placed a 732 ± 34 nm bandpass filter (Semrock) at the entrance of the emission monochromator in order to collect the signal at 700 nm without any interference from the second order diffraction of the excitation light or due to stray light. We assessed the positions of Q-bands by decomposing

Table 1 Specimens analyzed. Collection abbreviations: ZMB, Museum für Naturkunde of Berlin; JAGUARS, Cayenne collection; MNHN, Muséum national d'Histoire naturelle of Paris; NRM, Swedish Museum of Natural History of Stockholm; AH, Anthony Herrel personal collection; NKMP, Naturkundemuseum of Potsdam. Type of analysis conducted: UVL, macro-observation under UV lamp; EmS, emission spectroscopy; Ex-MI, excitation spectroscopy and multispectral imaging. Visible color of their fur observed under UV lamp: NF, no photoluminescence detected through macro-analysis. Porphyrin detection obtained with spectroscopy analysis: 0 = no, 1 = yes

| Mammal class	Order	Species	Specimen number	Type of analysis	Fur under UV	Porph.
Prototheria (egg-laying mammals)	Monotremata	*Ornithorhynchus anatinus* (Platypus)	ZMB_Mam_35 991	UVL, EmS	Green/cyan	0
Metatheria (marsupials)	Didelphimorphia	*Caluromys lanatus* (brown-eared woolly opossum)	ZMB_Mam_47 995	UVL	Pink	—
		Marmosa murina (Linnaeus' mouse opossum)	JAGUARS-M535	UVL, EmS, Ex-MI	Pink/red	1
		Marmosa murina (Linnaeus' mouse opossum)	MNHN 2001-1966	UVL	Pink	—
		Metachirus nudicaudatus (brown four-eyed opossum)	MNHN 1988-68	UVL	Pink	—
		Monodelphis brevicaudata (Guyanan short-tailed opossum)	JAGUARS-M2962	UVL, EmS, Ex-MI	Pink/red	1
		Monodelphis brevicaudata (Guyanan short-tailed opossum)	JAGUARS-M2838	UVL, EmS, Ex-MI	Pink/red	1
		Monodelphis brevicaudata (Guyanan short-tailed opossum)	MNHN 1995-3216	UVL	Pink	—
Eutheria (placentals)	Erinaceomorpha	*Erinaceus europaeus* (West European hedgehog)	NRM-MA594242	UVL, EmS, Ex-MI	Pink/red	—
		Erinaceus roumanicus (Northern white-breasted hedgehog)	ZMB_Mam_48 212	UVL	Pink/red	1
	Carnivora	*Mustela erminea* (Beringian ermine)	NKMP-unnumbered	UVL	Lavender	—
		Mustela erminea (Beringian ermine)	NRM-MA20175124	UVL, EmS	Lavender	0
		Vulpes lagopus (Arctic fox)	NRM-MA710029	UVL, EmS	NF	0
	Soricomorpha	*Crocidura russula* (greater white-toothed shrew)	AH, unnumbered	UVL, EmS	NF	0
		Talpa europaea (European mole)	AH, unnumbered	UVL, EmS	NF	0
	Lagomorpha	*Lepus timidus* (mountain hare)	NRM-MA588837	UVL, EmS	NF	0
	Rodentia	*Glaucomys volans* (southern flying squirrel)	ZMB_Mam_60 634	UVL, EmS, Ex-MI	Pink	1
		Glaucomys volans (southern flying squirrel)	MNHN 1939-707	UVL	Pink	—
		Glaucomys sabrinus (northern flying squirrel)	NRM-MA875246	UVL, EmS, Ex-MI	Pink	1
		Hylopetes spadiceus (red-cheeked flying squirrel)	MNHN 1979-368	UVL	Pink	—
		Pteromyscus pulverulentus (smoky flying squirrel)	MNHN–1979-376	UVL	Pink	—
	Chiroptera	*Plecotus auritus* (brown long-eared bat)	AH, unnumbered	UVL, EmS	NF	0
	Primates	*Mico argentatus* (silvery marmoset)	NRM-MA617493	UVL, EmS	NF	0
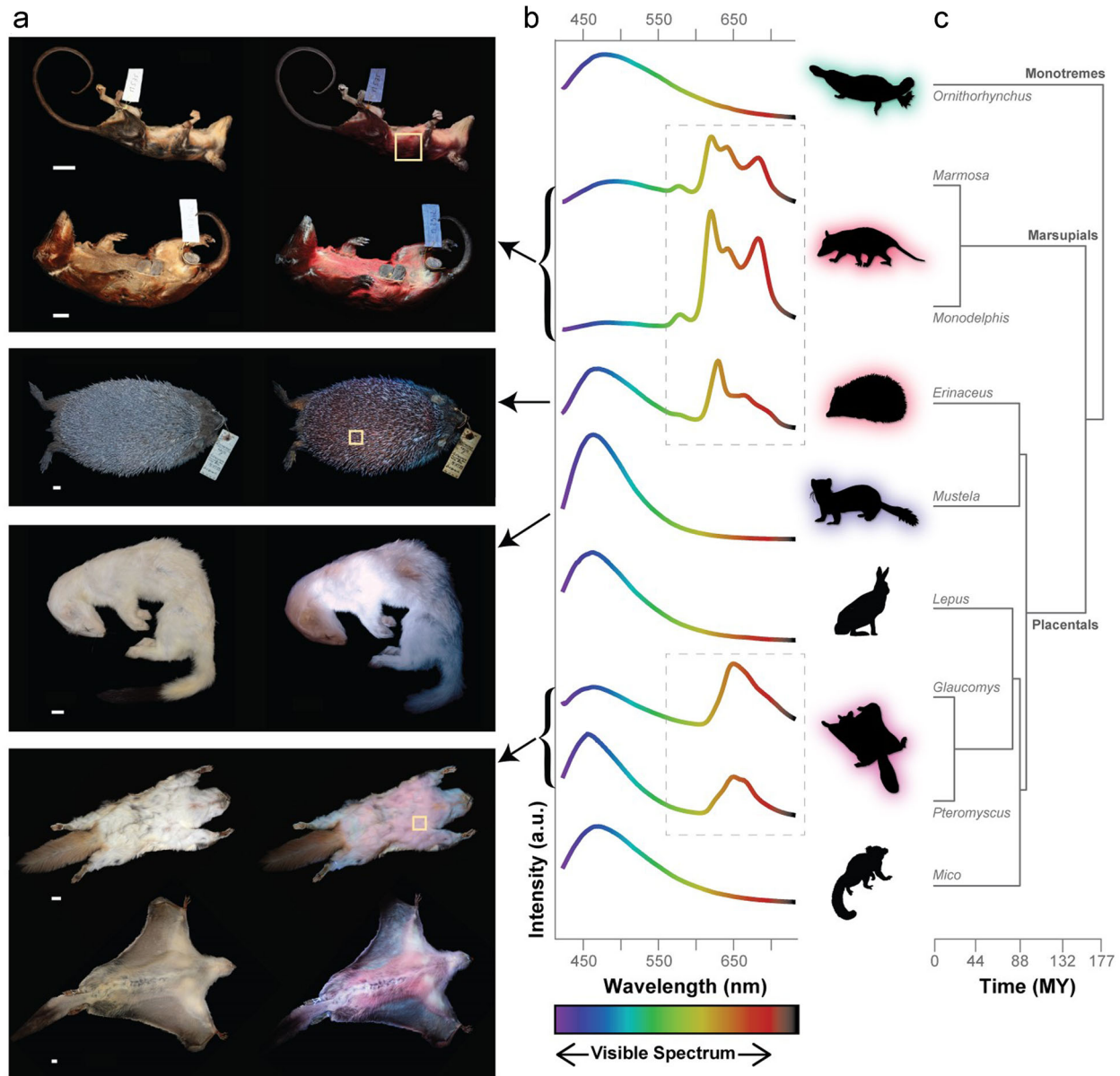
Figure 1 Illustration of UV-based photoluminescence of fur and spines in various mammal species. (a) Photographs of, from top to bottom: *Marmosa murina* JAGUARS-M535 (opossum), *Monodelphis brevicaudata* JAGUARS-M2962 (opossum), *Erinaceus roumanicus* ZMB_Mam_48 212 (hedgehog), *Mustela erminea* NKMP-unnumbered (ermine), *Glaucomys volans* MNHN 1939-707 (flying squirrel), and *Pteromyscus pulverulentus* MNHN–1979-376 (flying squirrel), under standard white light (left) and under controlled UV illumination (right). Scale bars = 1 cm. The yellow squares represent the localization of further multispectral imaging presented in Fig. 2. (b) Emission spectra obtained with luminescence spectroscopy technique on fur samples of, from top to bottom: *Ornithorhynchus anatinus* ZMB_Mam_35 991 (platypus), *Marmosa murina* JAGUARS-M535, *Monodelphis brevicaudata* JAGUARS-M2962, *Erinaceus europaeus* NRM-MA594242, *Mustela erminea* NRM-MA20175124, *Lepus timidus* NRM-MA588837 (hare), *Glaucomys volans* ZMB_Mam_60 634, *Glaucomys sabrinus* NRM-MA875246, and *Mico argentatus* NRM-MA617493 (primate). Glowing halos surrounding black silhouettes indicate the visible photoluminescent color of the fur only, observed from macro-analysis (see also Table 1). Black silhouettes are all public domain and from phylopic.org. (c) Phylogenetic relationships of the associated specimens (from timetree.org; Kumar *et al*. 2017) showing the widespread distribution of UV-based photoluminescence across mammals.
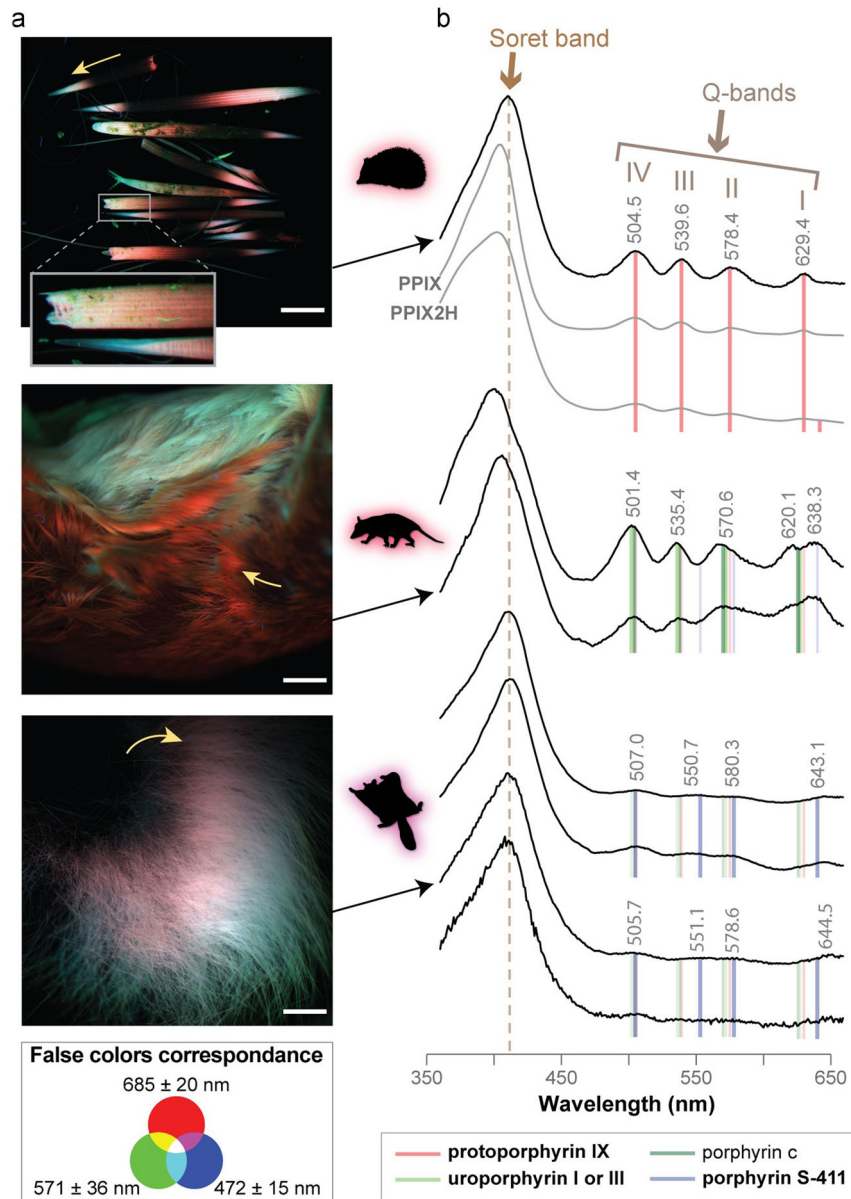
Figure 2 Characterization of the reddish photoluminescence of mammalian skin appendages. (a) False color multispectral images under 385 nm excitation of spines and hairs analyzed using spectroscopy, revealing a heterogeneous distribution of photoluminescent compounds into and along the spines of hedgehogs (including a magnified inset) and pelage and hairs of marsupials and flying squirrels. Sampling localizations are indicated by yellow squares in Fig. 1a. Arrows represent the direction of spine or hair growth. Scale bars = 3 mm. False colors correspond to the detected wavelengths (see the 3-color scale for correspondences). (b) All excitation spectra are characteristic of free-base porphyrins. Identifications of specific porphyrins, from top to bottom: Hedgehog's dorsal spines (*Erinaceus europaeus* NRM-MA594242), protoporphyrin IX (PPIX) and protonated protoporphyrin IX (PPIX2H) reference spectra, opossums' ventral fur from complete alcohol-preserved specimen (*Monodelphis brevicaudata* JAGUARS-M2838 above, and *Marmosa murina* JAGUARS-M535 below), a flying squirrel's ventral hair samples (*Glaucomys volans* ZMB_Mam_60 634) which appeared as glowing (above) and non-glowing (below) to the human eye under macro-imaging, and another flying squirrel's ventral and dorsal hair samples (*Glaucomys sabrinus* NRM-MA875246) which appeared as glowing (above) and non-glowing (below) to the human eye under macro-imaging. Position of the Q-bands is indicative of PPIX for the hedgehog, uroporphyrin for the marsupials, and porphyrin S-411 for the flying squirrels. Position of the Q-bands of porphyrin c, close to that of uroporphyrin, is also displayed for reference.

the Q-bands domain of each spectrum into a Gaussian distribution. The R script describing this procedure and the raw data necessary to reproduce the emission and excitation spectra are available at https://doi.org/10.6084/m9.figshare.14502105 and https://doi.org/10.6084/m9.figshare.14502114, respectively.

Photoluminescence multispectral imaging

We assembled false color luminescence images using black and white images collected with a custom-made setup that consisted of a low-noise 4-megapixel Si C-MOS camera (ORCA flash V4.0 V2–Hamamatsu) with a sensitivity for wavelengths between 200 and 1100 nm. The camera is fitted with a UV-VIS-IR 60 mm 1:4 Apo Macro lens (CoastalOptics) in front of which is positioned a filter wheel holding 8 interference band-pass filters (Semrock) to collect images in specific spectral ranges. We provided illumination using 16 LED lights emitting photons ranging from 365 up to 700 nm (CoolLED pE-4000) that were coupled to a liquid light-guide fiber fitted with a fiber-optic ring light-guide, allowing homogeneous illumination of the region of interest. We generated false color images by assigning red, green, and blue color to specific emission ranges using ImageJ software.

RESULTS AND DISCUSSION

Interspecific and intra-individual variation of UV-PL hues across mammals

Macroscopic examination of skins under long-wave UV illumination (365–395 nm) confirms the presence of conspicuous photoluminescence in a large number of mammalian species from all 3 major mammalian subclades (monotremes, marsupials, and placentals) (Fig. 1 and Table 1). Emission spectroscopy, which was used to achieve an unbiased characterization of the produced hues of luminescence, reveals that all analyzed specimens emit broadly in the blue region with varying intensities (see the broad band at 450–480 nm in Fig. 1b). This blue UV-PL is particularly noticeable to the human eye on the poorly pigmented pelage of hedgehogs, ermines, and flying squirrels (Fig. 1a). The UV-PL of the pelage of the platypus is shifted slightly toward green wavelengths, as previously reported (Anich et al. 2021). Emission spectroscopy also confirms that a pink to red UV-PL is exhibited by the skin appendages (hair and spines) of marsupials (opossums) and some of the placental mammals that we examined, the latter including flying squirrels

(Euarchontoglires) and hedgehogs (Laurasiatheria) (Table 1 and Fig. 1). The emission spectra obtained for these mammals' hair and spines feature a series of peaks (often 3) in the red region, between 600 and 690 nm, with variable intensity and position depending on the specimens (Fig. 1b). This suggests potential differences in the luminescing compounds or differences in the binding sites of these compounds (Sandberg et al. 1983). Furthermore, we observed that the localization of this reddish UV-PL on the pelage varies among species. In the specimens of opossums and flying squirrels studied, the belly was the body region that was most luminescent, while in hedgehogs it was the dorsal spines (Fig. 1a). Heterogeneous patterns of UV-PL distribution were also previously reported in flying squirrels and springhares (Kohler et al. 2019; Olson et al. 2021).

We further investigated the microscale localization of the reddish luminescing compounds using multispectral imaging under 385 nm (UV) excitation. Our false color images clearly reveal that these compounds are located within the spine and hair fibers of the mammals examined (Fig. 2a), as previously described in springhares (Olson et al. 2021). This is particularly noticeable in the hedgehog's spines, where the luminescent material, represented in shades of red in the false color images obtained from multispectral analysis, is located on the walls of the inner lumen of the spine (Fig. 2a). Furthermore, these compounds are not homogeneously distributed along the hair or spines or among individuals or species. In the hedgehog's spines, the luminescent material coats the walls of the inner lumen from base to apex. The regions that appear in white and shades of blue and green on the spectral images (see Fig. 2a) correspond to areas where the porphyrinic compounds are scarce or absent. The regions of the hair and spines that appear darker correspond to the more pigmented areas, suggesting that melanin content can hamper UV-PL observations. Additionally, in the hairs of marsupials and rodents we sampled, reddish luminescing compounds were present either along the entire length of the hair (marsupials) or restricted to a more basal region (flying squirrels).

In situ characterization of the reddish luminescing compounds

Using chromatography-mass spectrometry-based approaches, previous studies identified free base porphyrins as the compounds responsible for the pink to red luminescence of mammal pelage. Such approaches, however, only provide bulk information from extracts, leading to debates

about the exogenous or endogenous origin of the signal (Hamchand *et al.* 2021). We overcome this limitation by probing, directly on solid samples and *in situ*, the absorption properties of the pink to red luminescing compounds using excitation spectroscopy, a technique that produces spectra similar to absorption spectra by scanning the excitation wavelength at a fixed emission wavelength—here 700 nm corresponding to the observed red UV-PL. Contrary to emission spectroscopy, this methodology yields absorption-like spectra that are specific to certain compounds and can hence result in their precise identification. Spectra collected for the respective hair or spines show an intense band between 390 and 430 nm (the so-called Soret band), followed by a series of bands, ten to a hundred times less intense, between 480 and 660 nm (the so-called Q-bands), which are characteristic of free-base (non-metalated) porphyrins (e.g. DiNello & Chang 1978; Fig. 2b). An exhaustive identification of the complex mixture of compounds associated to porphyrins in the skin appendages of mammals would require the use of other methods such as high-performance liquid chromatography-mass spectrometry, which is out of the scope of the present work that focuses on the origin of the conspicuous reddish UV-PL observed in the skin appendages of mammals. Rather, our approach uniquely allows for the specific probing of this reddish UV-PL, within its *in situ* chemical environment, unambiguously ensuring that we identify the responsible compound(s) and not a wide range of other (non-luminescing) compounds that are not associated with the observed UV-PL.

The position, number, and band ratios of the Q-bands further allow for a robust identification of porphyrinic compounds (e.g. DiNello & Chang 1978). Q-bands of decreasing intensity at 504.5, 539.6, 578.4, and 630.1 nm are strongly indicative of protoporphyrin IX (PPIX) in the hedgehog's spines (Fig. 2b). The different position and number of bands for the hair of opossums and flying squirrels suggest the presence of other porphyrins. Following the DiNello and Chang (1978) database, the position of Q-bands at 501.4, 535.4, 570.5, and 619.6 nm in the opossums' hairs (Fig. 2b) is consistent with uroporphyrin I or III, and less likely with porphyrin c. The fifth band observed at 638.4 nm most likely indicates that the uroporphyrin is protonated, which is also supported by the shoulder on the Soret band, 2 modifications illustrated by our protonated protoporphyrin IX (PPIX2H) reference spectrum. For the flying rodents' hairs, the position of Q-bands at ~506, ~550, 578, and 640–646 nm only matches those of porphyrin S-411 (DiNello & Chang 1978), an analogue of the more common coproporphyrin (French *et al.* 1970).

The platypus and ermine likely have other photoluminescent compounds in their pelage that remain to be identified. The identification of the compounds responsible for these specific UV-PL colors (blue-green and lavender) will require investigation using other methods, because unlike free-base porphyrins, these compounds do not produce characteristic excitation spectra.

Is porphyrin in the skin appendages of mammals exogenous?

Hamchand *et al.* (2021) recently suggested that the porphyrins present in the European hedgehog's spines may have an exogenous origin. They analyzed the spine microbiome and identified several bacterial clades that could be responsible for the production of the porphyrins observed in the spines. This hypothesis deserves further scrutiny. The distribution of pigments we observed, with UV-PL restricted spatially to some regions of pelage in both the hedgehog's and other mammals' skin appendages, is not consistent with the activity of commensal bacteria propose by Hamchand *et al.* (2021). Furthermore, the latter study has identified qualitatively similar microbiomes on the surface of the hedgehog's spines and on the whole ground spines. This is also inconsistent with our observations, namely, that the porphyrinic compounds' distribution is restricted to the inner lumen of the spines. The distribution revealed by our multispectral imaging analysis rather suggests that the porphyrinic compounds were excreted within the skin appendages over the course of the natural process of continuous pelage growth. We thus view an endogenous origin of the porphyrins as a more plausible scenario. This hypothesis is further strengthened by pathological observations such as in one pet African hedgehog (*Atelerix*) described as excreting relatively large amounts of free-base porphyrins through both urine and feces, and which showed consistent reddish luminescence in its teeth, feet, and spines (Wolff *et al.* 2005).

Porphyrin accumulation into mammalian pelage is widespread

Our results also support that several distantly related mammals accumulate free-base porphyrins in their pelage. Reddish UV-PL, likely also indicative of porphyrin accumulation, is known in the pelage of additional species, including for instance most, if not all, members of Didelphimorphia (American marsupials) (Pine *et al.* 1985) and at least one species of Peramelemorphia (long-nosed bandicoot, *Perameles nasuta*) (Reinhold 2021).

Porphyrin accumulation in skin appendages may hence be quite widespread among mammals.

As part of the heme biosynthesis pathway, porphyrins are associated with all aerobic and anaerobic metabolisms and are ubiquitous in the cells of many organisms (Ajioka *et al*. 2006; de Oliveira Neves & Galván 2020). Protoporphyrins and their natural derivatives, like uroporphyrins and protoporphyrin S-411, are known to be photoluminescent and are also involved in coloration, for example, in the feathers of many birds (Church & Oxon 1869; Rimington 1939; Negro *et al*. 2009; Galván *et al*. 2016; Camacho *et al*. 2019; Okazaki & Imamura 2019). Interestingly, although protoporphyrins are normally excreted through feces in mammals, their overproduction and tissue accumulation has also been shown to be associated with diseases known as erythropoietic protoporphyrias. Other inherited metabolic porphyria disorders—described in humans with accumulation of δ-aminolevulinic acid and porphobilinogen—cause neurovisceral attacks (acute hepatic porphyrias), or/and skin lesions (cutaneous porphyrias with accumulation of porphyrin ring structures) depending on the heme biosynthetic pathway step affected (Kauppinen 2005; Karim *et al*. 2015). In addition to occurring in humans, this condition has been described in a few other mammals such as ruminants, horses, and cats (Rimington & Moore 1985; Tennant 1998). Interestingly, several cases of protoporphyrin accumulation not causing disease have also been reported in mammals. Notably, fox squirrels (*Sciurus niger*) are known to accumulate the free-base uroporphyrin I in their internal organs and skin without showing detrimental symptoms, as a result of the low activity of the enzyme uroporphyrinogen III synthase (de Oliveira Neves & Galván 2020). Other freebase porphyrins were recently identified as responsible for a non-pathological conspicuous reddish UV-PL on the pelage of several springhare species (Olson *et al*. 2021). Non-pathological porphyrin accumulation in the African hedgehog (*Atelerix*) was also corroborated by a survey of 55 healthy, captive individuals observed under UV light (Silpa *et al*. 2021).

As our analyses were conducted on preserved museum specimens, we could not determine whether these individuals exhibited porphyria symptoms in life, nor could we assess exactly how they accumulated porphyrin in their hair. Nonetheless, previous observations on living individuals suggest that this condition is generally harmless in most mammal species (Wolff *et al*. 2005; de Oliveira Neves & Galván 2020; Olson *et al*. 2021).

We suspect that the blue UV-PL we observed in all examined mammals (including those for whom porphyrins were not detected) is likely due at least in part to the hair keratins. Low pigmented human hair is known to photoluminesce into the human visible spectrum under UV in the 450–480 nm range due to this family of structural proteins (Millington & Marsh 2019). While melanins also luminesce in this broad region of the spectrum (Gallas & Eisner 1987; Hamchand *et al*. 2021), this would not explain the spectrum obtained for the winter coat ermine (Fig. 1a,b) and other poorly pigmented hair.

Does pelage photoluminescence have a function?

As the reddish UV-PL is predominantly found in crepuscular and nocturnal species, this phenomenon has been interpreted as potentially related to visual functions for intraspecific communication or camouflage in light-deprived environments (Camacho *et al*. 2019; Kohler *et al*. 2019; Anich *et al*. 2021; Olson *et al*. 2021). However, in showing that the reddish UV-PL of mammals' pelage is caused by the accumulation of porphyrins, which are photodegradable compounds, it appears more likely that the overrepresentation of UV-PL in crepuscular and nocturnal species is simply the result of the lower degree of degradation of porphyrinic compounds in these taxa compared to diurnal species. Furthermore, it should be kept in mind that it is far from evident that natural UV illuminating sources, even at dusk or dawn, would be sufficient to elicit detectable UV-PL distinguishable from natural ambient visible light to permit its perception by either co-specifics or predators (Goutte *et al*. 2019). It is irrelevant whether or not the latter have short-wavelength sensitive cone based blue vision, or medium to long wavelength sensitive cone based yellow/red vision, because UV-PL emission will always be dominated by the elastic scattering (reflectance) of photons from the same spectral domain. Additionally, we emphasize that the reemitted light of the UV-PL discussed here is in the orange and red spectral domain (600–700 nm). Therefore, whether the animals have an improved UV light vision, generally in the 315–400 nm domain (Cronin & Bok 2016), does not provide them with any advantage in the perception of such photoluminescence.

We suggest an alternative hypothesis to explain the accumulation of free-base porphyrins in the pelage of mammals, resulting in this observable UV-PL. This phenomenon might simply be a byproduct of the heme biosynthesis pathway with no other function than the excretion in inert material of porphyrins produced in the body (Lagorio *et al*. 2015; Marshall & Johnsen 2017). Indeed, storing these residual molecules of the heme pathway—which become toxic when produced in too high quantities and are photoreactive (Kauppinen 2005; Ajioka *et al*. 2006; Karim *et al*. 2015)—in skin appendages that

consist of inert tissues such as hair or spines and that are exposed to light, could assist in the excretion of these compounds from the body. As dermal lesions in humans tend to be found in areas of the skin where hair is sparse (Karim *et al.* 2015), accumulating porphyrins in the inert hair or spine could help circumvent issues associated with keeping them in living tissues that are exposed to light such as the skin, together with accumulating them in internal organs where this is more tolerable (de Oliveira Neves & Galván 2020). Understanding the significance of the distribution of porphyrins at the scale of the whole pelage (spread evenly vs. concentrated in some specific anatomical regions) will require an analysis involving a systematic sampling of the pelage of living or recently deceased animals (to account for potential preservation biases).

Porphyrin preservation in museum specimens

We found that UV-PL is less intense in areas that are less pigmented and in hairs that are thinner (e.g. flying squirrels) compared to the thicker and more pigmented spines of hedgehogs (Fig. 2a). Additionally, we found that alcohol-preserved specimens (e.g. the marsupials from the JAGUARS collections) show higher intensity of UV-PL compared to the dry-preserved specimens of hedgehog or flying squirrels. Variation of reddish UV-PL intensity in dry-preserved museum specimens was also previously noted by Pine *et al.* (1985), Kohler *et al.* (2019), and Olson *et al.* (2021). Because porphyrins are photodegradable compounds (Poh-Fitzpatrick & DeLeo 1977), it seems likely that the preservation of the reddish UV-PL on the specimens' pelage may be affected by both the preservation method employed and the amount of light they have been exposed to through time. Hence, one should not draw the conclusion that a given species does not accumulate porphyrins in its pelage based solely on the apparent lack of UV-PL in some museum specimens. This further supports that porphyrin accumulation in the pelage of mammals might be much more common than previously assumed.

CONCLUSIONS

We showed that distantly related mammals display pelage with reddish UV-PL that can be ascribed to the presence of free-base porphyrins within their hair or spines. Understanding the exact process responsible for the presence of these compounds in the skin appendages of mammals will require further investigation, but given the data at hand, we suspect that it is unlikely

that such luminescence was acquired in the context of inter-individual communication or camouflage. The presence of porphyrins in the pelage of mammals could be purely incidental, but we present an alternative hypothesis that involves deposition of these compounds in skin appendages as a complementary mean of excreting them, hence avoiding dermal lesions. Further research on the functional significance of UV-induced photoluminescence in animals and plants will require more thorough and comprehensive approaches, incorporating aspects of both the ecology and physiology of the organisms exhibiting these phenotypes (Lagorio *et al.* 2015; Marshall & Johnsen 2017). Because photoluminescence spectroscopy and multispectral imaging can be used for *in situ* analyses and at various time scales, these methods have the potential to help answer emerging questions about spatial and temporal distribution of compounds such as free-based porphyrins.

REFERENCES

Ajioka RS, Phillips JD, Kushner JP (2006). Biosynthesis of heme in mammals. *Biochimica et Biophysica Acta - Molecular Cell Research* **1763**, 723–36.

Anich PS, Anthony S, Carlson M *et al.* (2021). Biofluorescence in the platypus (*Ornithorhynchus anatinus*). *Mammalia* **85**, 179–81.

Arnold KE, Owens IPF, Marshall NJ (2002). Fluorescent signaling in parrots. *Science* **295**, 92.

Bachman CH, Ellis EH (1965). Fluorescence of bones. *Nature* **206**, 1328–31.

Camacho C, Negro JJ, Redondo I, Palacios S, Sáez-Gómez P (2019). Correlates of individual variation in the porphyrin-based fluorescence of red-necked nightjars (*Caprimulgus ruficollis*). *Scientific Reports* **9**, 19115.

Church AH, Oxon MA (1869). Researches on Turacin, an animal pigment containing copper. *Philosophical Transactions of the Royal Society of London* **159**, 627–36.

Cronin TW, Bok MJ (2016). Photoreception and vision in the ultraviolet. *Journal of Experimental Biology* **219**, 2790–801.

de Oliveira Neves AC, Galván I (2020). Models for human porphyrias: Have animals in the wild been overlooked?: Some birds and mammals accumulate significant amounts of porphyrins in the body without showing the injurious symptoms observed in human porphyrias. *BioEssays* **42**, 2000155.

Derrien E, Turchini J (1925). Nouvelles observations de fluorescences rouges chez les animaux. *Compte rendu des séances de la Société de Biologie et de ses Filiales (Paris, France)* (September), 1030–1.

DiNello RK, Chang CK (1978). Isolation and modification of natural porphyrins. In: Dolphin D, ed. *The Porphyrins*. Academic Press, New York. pp. 289–339.

French J, Nicholson DC, Rimington C (1970). Identification of the acrylate porphyrin S-411 from meconium. *Biochemical Journal* **120**, 393–7.

Gallas JM, Eisner M (1987). Fluorescence of melanin-dependence upon excitation wavelength and concentration. *Photochemistry and Photobiology* **45**, 595–600.

Galván I, Camarero PR, Mateo R, Negro JJ (2016). Porphyrins produce uniquely ephemeral animal colouration: A possible signal of virginity. *Scientific Reports* **6**, 39210.

Goutte S, Mason MJ, Antoniazzi MM (2019). Intense bone fluorescence reveals hidden patterns in pumpkin toadlets. *Scientific Reports* **9**, 5388.

Hamchand R, Lafountain AM, Büchel R *et al.* (2021). Red fluorescence of European hedgehog (*Erinaceus europaeus*) spines results from free-base porphyrins of potential microbial origin. *Journal of Chemical Ecology* **47**, 588–96.

Hughes B, Bowman J, Stock NL, Burness G (2022). Using mass spectrometry to investigate fluorescent compounds in squirrel fur. *PLoS ONE* **17**, e0257156.

Jeng M-L (2019). Biofluorescence in terrestrial animals, with emphasis on fireflies: A review and field observation. In: Suzuki H, ed. *Bioluminescence–Analytical Applications and Basic Biology*. IntechOpen, London, pp. 1–15.

Karim Z, Lyoumi S, Nicolas G, Deybach JC, Gouya L, Puy H (2015). Porphyrias: A 2015 update. *Clinics and Research in Hepatology and Gastroenterology* **39**, 412–25.

Kauppinen R (2005). Porphyrias. *Lancet* **365**, 241–52.

Kellie A, Dain SJ, Banks PB (2004). Ultraviolet properties of Australian mammal urine. *Journal of Comparative Physiology A: Neuroethology, Sensory, Neural, and Behavioral Physiology* **190**, 429–35.

Kohler AM, Olson ER, Martin JG, Anich PS (2019). Ultraviolet fluorescence discovered in New World flying squirrels (*Glaucomys*). *Journal of Mammalogy* **100**, 21–30.

Kumar S, Stecher G, Suleski M, Hedges SB (2017). TimeTree: A resource for timelines, timetrees, and divergence times. *Molecular Biology and Evolution* **34**, 1812–9.

Lagorio M, Cordon G, Iriel A (2015). Reviewing the relevance of fluorescence in biological systems. *Photochemical and Photobiological Sciences* **14**, 1538–59.

Latham R (1953). Simple method for identification of least weasel. *Journal of Mammalogy* **34**, 385.

Leiner MJP, Hubmann MR, Wolfbeis OS (1987). The total fluorescence of human urine. *Analytica Chimica Acta* **198**, 13–23.

Lim MLM, Land MF, Li D (2007). Sex-specific UV and fluorescence signals in jumping spiders. *Science* **315**, 481.

Marshall J, Johnsen S (2017). Fluorescence as a means of colour signal enhancement. *Philosophical Transactions of the Royal Society B: Biological Sciences* **372**, 20160335.

McGraw KJ, Toomey MB, Nolan PM, Morehouse NI, Massaro M, Jouventin P (2007). A description of unique fluorescent yellow pigments in penguin feathers. *Pigment Cell Research* **20**, 301–4.

Meisner DH (1983). Psychedelic opossums: fluorescence of the skin and fur of *Didelphis virginiana*. *The Ohio Journal of science* **83**, 4.

Millington KR, Marsh JM (2019). Anomalous fluorescence of white hair compared to other unpigmented keratin fibres. *International Journal of Cosmetic Science* **42**, 289–301.

Moncrief ND, Dooley AC (2013). Using fluorescence of bones and teeth to detect remains of the Eastern fox squirrel (*Sciurus niger*) in archaeological deposits. *Southeastern Archaeology* **32**, 46–53.

Negro JJ, Bortolotti GR, Mateo R, García IM (2009). Porphyrins and pheomelanins contribute to the reddish juvenal plumage of black-shouldered kites. *Comparative Biochemistry and Physiology - B Biochemistry and Molecular Biology* **153**, 296–9.

Okazaki T, Imamura S (2019). Distribution of protoporphyrin IX in bird feathers. *International Journal of Analytical Bio-science* **7**, 41–8.

Olson ER, Carlson MR, Ramanujam VMS *et al*. (2021). Vivid biofluorescence discovered in the nocturnal Springhare (Pedetidae). *Scientific Reports* **41**, 4125.

Pearn SM, Bennett ATD, Cuthill IC (2001). Ultraviolet vision, fluorescence and mate choice in a parrot, the budgerigar *Melopsittacus undulatus*. *Proceedings of the Royal Society B: Biological Sciences* **268**, 2273–9.

Pine RH, Rice JE, Bucher JE, Tank DH, Greenhall AM (1985). Labile pigments and fluorescent pelage in didelphid marsupials. *Mammalia* **49**, 249–56.

Poh-Fitzpatrick MB, DeLeo VA (1977). Rates of plasma porphyrin disappearance in fluorescent vs. red incandescent light exposure. *The Journal of Investigative Dermatology* **69**, 510–2.

Prötzel D, Heß M, Scherz MD, Schwager M, Padje AV, Glaw F (2018). Widespread bone-based fluorescence in chameleons. *Scientific Reports* **8**, 698.

Prötzel D, Heß M, Schwager M, Glaw F, Scherz MD (2021). Neon-green fluorescence in the desert gecko *Pachydactylus rangei* caused by iridophores. *Scientific Reports* **11**, 297.

Pynne JT, Castleberry SB, Conner LM *et al*. (2021). Ultraviolet biofluorescence in pocket gophers. *Midland Naturalist* **186**, 150–5.

Reinhold L (2021). Mammals with fluorescent fur: Observations from the wet tropics. *North Queensland Naturalist* **51**, 1–8.

Rimington C (1939). A reinvestigation of turacin, the copper porphyrin pigment of certain birds belonging to the Musophagidae. *Proceedings of the Royal Society B* **127**, 106–20.

Rimington C, Moore MR (1985). Porphyria in animals. *Clinics in Dermatology* **3**, 144–55.

Sandberg S, Talstad I, Hovding G, Bjelland N (1983). Light-induced release of protoporphyrin, but not of zinc protoporphyrin, from erythrocytes in a patient with greatly elevated erythrocyte protoporphyrin. *Blood* **62**, 846–51.

Silpa MAC, Mclaughlin A, Music, Strunk A (2021). Ultraviolet light induced fluorescence in the captive African pygmy hedgehog (*Atelerix* spp.). In: Hackeman M, Dox W, Lombardo T, Glickman S, eds. *ExoticsCon Conference Proceedings*; 28 Aug–2 Sep 2021, Nashville TN, United States. ExoticsCon, pp. 356–7.

Taboada C, Brunetti AE, Pedron FN *et al*. (2017). Naturally occurring fluorescence in frogs. *PNAS* **114**, 3672–7.

Tahoun M, Gee CT, McCoy VE, Sander PM, Müller CE (2021). Chemistry of porphyrins in fossil plants and animals. *RSC Advances* **11**, 7552–63.

Tennant BC (1998). Lessons from the porphyrias of animals. *Clinics in Dermatology* **16**, 307–15.

Tumlison CR, Tumlison T (2021). Investigation of fluorescence in selected mammals of Arkansas. *Journal of the Arkansas Academy of Science* **75**, 29–35.

Weidensaul CS, Colvin BA, Brinker DF, Huy JS (2011). Use of ultraviolet light as an aid in age classification of owls. *Wilson Journal of Ornithology* **123**, 373–7.

Wolff CF, Corradini PR, Galaxia CLMV (2005). Congenital erythropoietic porphyria in an African hedgehog (*Atelerix albiventris*). *Journal of Zoo and Wildlife Medicine* **36**, 323–5.

Cite this article as: